Journal of Magnetics 11(4), 189-194 (2006)

<Invited review paper>

Substrate-free Biosensing using Brownian Rotation of Bio-conjugated Magnetic Nanoparticles

Seok-Hwan Chung[1,2,†*], Axel Hoffmann[1,2], Liaohai Chen[3], Shouheng Sun[4], Konstantin Guslienko[1,‡], Marcos Grimsditch[1], and Samuel D. Bader[1,2]

[1]Materials Science Division, [2]Center for Nanoscale Materials,
[3]Bioscience Division, Argonne National Laboratory, Argonne, IL 60439, USA
[4]Department of Chemistry, Brown University, Providence, Rhode Island 02912, USA
[†]Current Address: Center for Nanoscale Science and Technology, National Institute of Standards and Technology, Gaithersburg, MD 20899, USA
[‡]Current Address: Research Center for Spin Dynamics and Spin-Wave Devices, Department of Materials Science and Engineering, Seoul National University, Korea

(Received 14 November 2006)

The recent development of bio-conjugated magnetic nanoparticles offers many opportunities for applications in the field of biomedicine. In particular, the use of magnetic nanoparticles for biosensing has generated widespread research efforts following the progress of various magnetic field sensors. Here we demonstrate substrate-free biosensing approaches based on the Brownian rotation of ferromagnetic nanoparticles suspended in liquids. The signal transduction is through the measurement of the magnetic *ac* susceptibility as a function of frequency, whose peak position changes due to the modification of the hydrodynamic radius of bio-conjugated magnetic nanoparticles upon binding to target bio-molecules. The advantage of this approach includes its relative simplicity and integrity compared to methods that use substrate-based stray-field detectors.

Keywords : *ac* susceptibility, Brownian relaxation, magnetic nanoparticle, biomagnetic sensor

1. Introduction

There has recently been an increased interest in magnetic nanoparticles due to both fundamental scientific research and potential applications, such as in magnetic data storage, actuators and sensors [1]. Magnetic nanoparticles, either ferromagnetic or superparamagnetic, can also be conjugated with biological surfactants via layer-by-layer electrostatic assembly [2], encapsulation in polymer matrices [2], or material growth in protein-capsid templates [3]. These bio-conjugated magnetic nanoparticles generate opportunities for applications in many biomedical fields [4], such as targeted drug delivery, magnetic purification or separation, magnetic hyperthermia and contrast enhancement of magnetic resonance imaging (MRI). In particular, the use of magnetic labels for sensing applications has been the subject of extensive research efforts due to their advantages over other types of biosensors [5, 6]. The strong interaction between magnetic nanoparticles and an external magnetic field enables manipulation and sensitive detection of those particles for such sensor applications. Furthermore, the shelf-life of magnetic nanoparticles can be long compared to that of other materials for biosensing, such as fluorescent and radioactive materials.

In most biomagnetic sensing schemes, the basic idea is similar to that of conventional immunoassay techniques. Magnetically labeled biomolecules are cross-linked to a substrate via target molecules. The biological affinity selection includes the complementary bindings of ligand-receptor, antibody-antigen, or complementary DNA chains. After washing-off unbound molecules the presence of an immobilized target is verified via the detection of the magnetic stray field by means of substrate-based sensors, such as giant magnetoresistance [7], anisotropic magnetoresistance [8], tunneling magnetoresistance [9], Hall effect [10], fluxgate [11] or superconducting quantum interference (SQUID) devices [12, 13]. An alternative substrate-free sensing approach, which was proposed by Connolly and

*Corresponding author: Tel: +1-301-975-3768,
Fax: +1-301-926-2746, e-mail: shchung@mail.nist.gov

St. Pierre [14], relies on detecting the modification of the Brownian rotation of magnetic nanoparticles [15] when they bind to selective targets in liquid solution [16, 17].

In this work we discuss our recent results of utilizing the Brownian rotation of bio-conjugated magnetic nanoparticles in liquid for substrate-free biosensors. We used dynamic magnetic susceptibility as a function of frequency of the applied *ac* magnetic field to demonstrate the proof-of-principle of the biosensing scheme. Both magneto-electric and magneto-optic techniques were adapted for the *ac* susceptibility measurement. Compared to the more conventional substrate-based detection, only one binding event for each target molecule is required and the additional information such as sensor integrity and the size of target molecules can be obtained through this substrate-free approach.

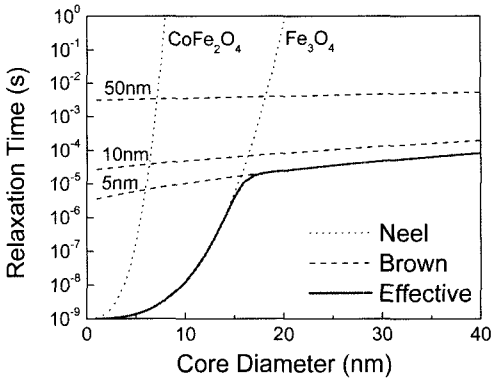

Fig. 1. Relaxation times of nanoparticles as a function of magnetic core diameter. Dotted lines are Néel relaxation time for $CoFe_2O_4$ and Fe_3O_4 magnetic cores. Dashed lines are Brownian relaxation for magnetic particles with different non-magnetic surfactant thicknesses in aqueous solution. The solid line is the effective relaxation time for Fe_3O_4 nanoparticle with a 5-nm surfactant shell.

2. Theory and Experiment

Nanoparticles (coated with a surfactant) suspended in a liquid exhibit both random rotational diffusive motion and translational motion due to thermal fluctuations. For the rotational diffusion (Brownian relaxation) of bio-conjugated magnetic nanoparticles with magnetic core radius r and surfactant shell thickness t, the relaxation time is given by: [18, 19]

$$\tau_B = \frac{4\pi\eta(r+t)^3}{k_B T}, \tag{1}$$

where η is the dynamic viscosity of the liquid and T is temperature. For small particles with small enough relative energy barrier, the magnetic moment directions within particles themselves can be changed due to the thermal fluctuations. This is called Néel relaxation and the corresponding relaxation time can be expressed as:

$$\tau_N = \tau_0 \exp\left(\frac{\Delta E}{k_B T}\right), \tag{2}$$

where τ_0 is generally on the order of 10^{-9}-10^{-10} sec and ΔE is an energy barrier, which depends on the magnetic anisotropy constant and the particle's magnetic volume. Since the Brownian and Néel relaxation processes are almost independent of each other, the effective relaxation rate is given as $\tau_{eff}^{-1} = \tau_B^{-1} + \tau_N^{-1}$. Figure 1 shows the Brownian, Néel, and effective relaxation times as a function of magnetic core diameter for cobalt ferrite ($CoFe_2O_4$) and magnetite (Fe_3O_4) nanoparticles with different surfactant shell thicknesses. The effective relaxation depends strongly on the particle's hydrodynamic size for the Brownian regime, and the particle's magnetic size and magnetic anisotropy for the Néel regime. Notice that compared to bulk material the anisotropies are generally higher and the saturation magnetizations tend to be lower due to surface and finite-size effects for nanoparticles [20].

For magnetic nanoparticles with large enough magnetic core size, the magnetization is blocked inside the nanoparticle. Therefore, in this case, the Brownian relaxation in the frequency domain can be measured directly by the imaginary part of the *ac* magnetic susceptibility as a function of frequency ω expressed as: [14]

$$\chi''(\omega) = \frac{\chi_0(\omega\tau)}{1+(\omega\tau)^2}, \tag{3}$$

where χ_0 is the static susceptibility and τ is the effective relaxation time of the nanoparticles. Note that χ'' has a maximum when $\omega = 1/\tau$. For nanoparticles with polydispersity, Eq. (3) should become an integral over the particle size distribution function [19].

For the experimental demonstration of the biosensing scheme we used avidin-coated magnetite (Fe_3O_4) nanoparticles [21] and water-soluble cobalt ferrite ($CoFe_2O_4$) nanoparticles. For the biological measurements, the nanoparticle sample was diluted with phosphate buffer saline (PBS, pH = 7.0) solution. The magnetic hysteresis and *ac* magnetic susceptibility of a 100-μl aliquot of the solution were measured in a Physical Property Measurement System (PPMS) [22]. The PPMS uses a magneto-electric scheme for *ac* magnetic susceptibility measurement. It detects the amplitude and phase of the sample's magnetic response using two detection coils while applying a small *ac* magnetic field to the sample with an *ac* drive and compensation coils. The field frequency was varied between 10

Hz and 10 kHz and an *ac* field amplitude of 10 Oe was applied for all the measurements. We also used a magneto-optic method [23] for the *ac* susceptibility measurement. This technique is based on the detection of the rotation of linearly polarized light upon transmission through an optically anisotropic colloidal suspension of magnetic nanoparticles. We used the *ac* susceptibility determined magneto-optically as a function of the frequency (10 Hz~5 kHz) of an *ac* applied magnetic field (10 Oe) to verify that the results agree with those obtained via the commercial PPMS.

3. Results and Discussion

A room temperature magnetization curve of avidin-coated Fe_3O_4 nanoparticles diluted with PBS solution exhibits paramagnetic behavior, as shown in Fig. 2. The transmission electron microscope (TEM) image of a nanoparticle, in the inset, shows a Fe_3O_4 core (the darkest contrast) of ~10 nm diameter covered by a 20-30 nm thick avidin shell. The particle concentration in the fluid was ~6 mg/ml (~2×10^{15} particles/ml). The paramagnetic behavior (zero remanence, zero coercivity) in Fig. 2 is due to single-domain nanoparticles rotating freely in the liquid in order to align with the external magnetic field. The magnetic moment of each nanoparticle can be estimated by fitting, the magnetization curve to the classic Langevin model given by:

$$M = M_s\left[\coth\left(\frac{mH}{k_BT}\right) - \frac{k_BT}{mH}\right], \quad (4)$$

where M_s is the saturation magnetization and m is the magnetic moment of each particle. From this fit the magnetic moment for each nanoparticle is 2.0×10^4 μ_B, which corresponds well to the value 2.8×10^4 μ_B estimated for a spherical single-domain magnetite nanoparticle with 10-nm diameter (using the bulk value for magnetite of M_s = 480 G).

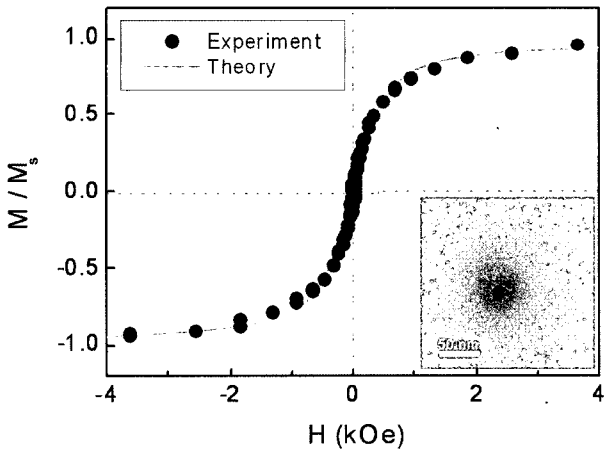

Fig. 2. Normalized magnetization of avidin-coated Fe_3O_4 nanoparticles in a PBS solution at room temperature as a function of applied magnetic field. Solid line is a calculated fit to the Langevin function. The inset shows a TEM image of the nanoparticle. Adapted from Ref. [19].

Figure 3 shows the real and imaginary part of the *ac* susceptibility as a function of frequency measured magneto-electrically using the PPMS and also magneto-optically. The sample was a mixture of aqueous solution of 14-nm $CoFe_2O_4$ nanoparticles (10 μl) and 50% polyethylene glycol (PEG) (190 μl), which corresponds to about 2×10^{12} nanoparticles. The dipolar interaction between magnetic nanoparticles was negligible due to their low volume fraction (12 ppm) and the large inter-particle distances. For the magnetic *ac* susceptibility measurements with the PPMS, a modulation field of 10 Oe was applied in the frequency range between 10 Hz and 10 kHz. The magneto-optic data has a good correspondence to the data acquired by the PPMS (see Fig. 3). The peak frequency of the imaginary part of the *ac* susceptibility and the corresponding inflection frequency of the real part in both sets of experimental data are the same. Furthermore, the technique detects much fewer particles (within a confined region of beam path) in a relatively short time.

Figure 4 shows the imaginary part of the *ac* susceptibility of the avidin-coated magnetite nanoparticles as a function of frequency. At room temperature there is a peak in the *ac* susceptibility at 210 Hz. However, the peak

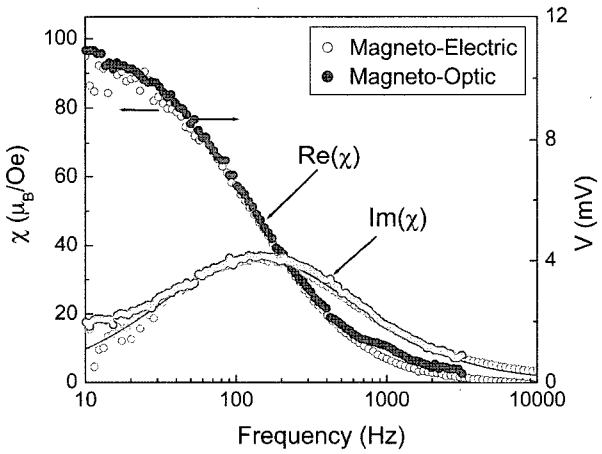

Fig. 3. Real and imaginary part of the *ac* magnetic susceptibility as a function of frequency for a mixture of aqueous solution of $CoFe_2O_4$ nanoparticles (10 μl) and a composition of water (160 μl) and 50% polyethylene glycol (PEG) (20 μl). Open symbols correspond to the measurements with a commercial magneto-electric setup (PPMS), and the experimental points measured with the magneto-optic setup are shown by solid symbols.

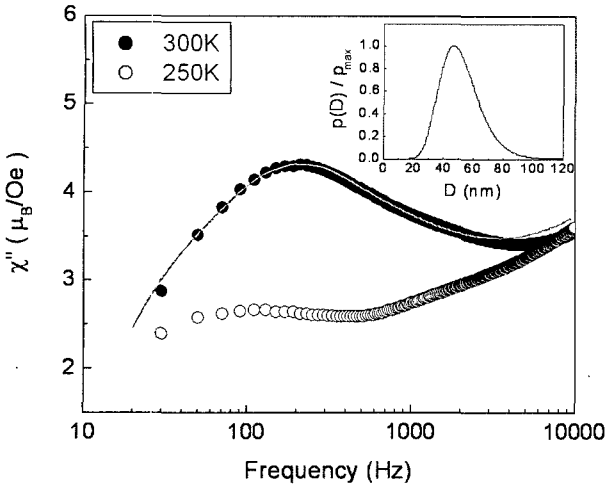

Fig. 4. Imaginary part of the *ac* magnetic susceptibility as a function of frequency for avidin-coated magnetic particles suspended in a PBS solution. Solid symbols correspond to the measurements at 300 K, open symbols - at 250 K, which is below the freezing point of the carrier liquid. Solid line is a fit using a convolution of Eqs. (3) and (5) and utilizing the 250-K data as background. The inset shows the log-normal size distribution used for the best fit. Adapted from Ref. [19].

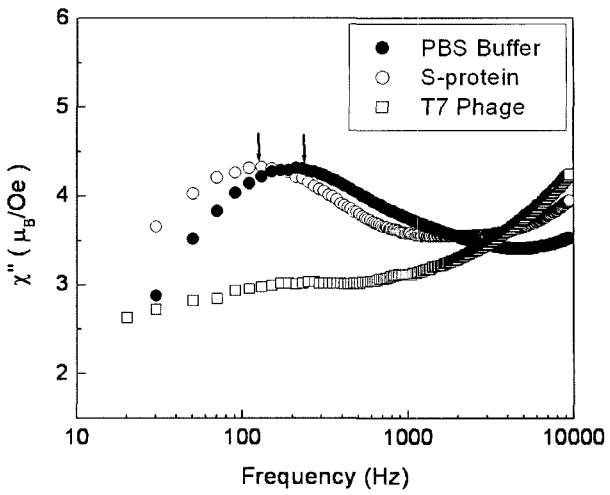

Fig. 5. Imaginary part of the *ac* magnetic susceptibility of an avidin-coated magnetic particle before (solid circles), after (open circles) binding to S-protein, and after (open squares) binding to biotinylated T7 bacteriophage. Adapted from Ref. [19].

disappears when the PBS solution is cooled below its freezing point (> 250 K). Since the freezing of the liquid immobilizes the nanoparticles at 250 K, this implies that the low frequency peak at room temperature is mainly due to the Brownian relaxation of the magnetization. The solid line shows a fit to a model that takes the size dispersion of the particles into account. Most nanoparticle systems have a log-normal size distribution given by [24]:

$$P(r) = \frac{1}{\sqrt{2\pi}\sigma_r} \exp\left[-\frac{(\ln r - \ln r_m)^2}{2\sigma_r^2}\right], \qquad (5)$$

where r_m is the median hydrodynamic radius, and σ_r is the standard deviation of *ln r*. A fit to the convolution of Eqs. (3) and (5) [19] using the 250-K data as a background suggests a ± 12% (σ_r = 0.26) distribution of the hydrodynamic radius of the nanoparticles that exhibit the Brownian relaxation. Notice that the size distribution for the magnetic core radii can be significantly wider. The inset of Fig. 4 shows the log-normal size distribution function for the best fit. Note that the high frequency responses at the two different temperatures are similar regardless of the presence of the low frequency peak. This is probably due to the existence of some unblocked superparamagnetic particles, since the median diameter of the magnetic core (~10 nm) is near to the crossover between the Brownian and Néel-dominated relaxation regimes [15].

In order to demonstrate the biosensing scheme, we added commercially available biotinylated S-protein [25] to the avidin-coated magnetite nanoparticle solution. The specific interaction of biotin and avidin protein has been well characterized in the literature with a large affinity constant on the order of a femtomole [26]. When biotinylated S-protein is added to the avidin-coated magnetite nanoparticles, the peak frequency decreases from 210 to 120 Hz, as shown in Fig. 5. Since S-protein does not exhibit any magnetic properties, this frequency shift has to be induced by the increased hydrodynamic size of the nanoparticles due to the interaction of biotinylated S-protein with the avidin-coated magnetic nanoparticles. Since Eq. (3) has a maximum when $\varpi = 1/\tau$, the peak frequency of the *ac* magnetic susceptibility is inversely proportional to the particle volume ($\omega_p \propto 1/r^3$). Assuming the median diameter of the avidin-coated magnetite particles is ~50 nm, as determined from the TEM measurements, this relation implies that the total particle diameter (core + shell) after S-protein binding is ~60 nm. Such size increase corresponds well to the size of the S-protein (~4 nm). This result demonstrates the feasibility of using the frequency peak of the *ac* susceptibility to monitor the attachment of a target molecule to magnetic nanoparticles, and even to obtain information about the size of the target molecule. This approach thus provides a bio-sensing scheme that uses the Brownian relaxation of magnetic nanoparticles in a liquid.

To further test the biosensing scheme, we pretreated the biotinylated S-protein with S-peptide displayed T7 bac-

Table 1. Comparison of the different biosensing schemes based on (i) magnetoresistance and Hall effects, (ii) SQUID, and (iii) new substrate-free detection using the Brownian relaxation of magnetic nanoparticles.

	MR and Hall Sensor	SQUID Sensor	Substrate-free Sensor
Number of Bindings	2	1 or 2	1
Sensitivity	Low-Mid	High	Mid
Sensing Target Size	No	No	Yes
Magnetic Separation after Sensing	No	Maybe	Yes
Portable Device	Yes	No	Yes

teriophage particles so that the biotinylated S-protein will be anchored to the surface of the T7 bacteriophage due to the specific interaction between the S-peptide and S-protein. Subsequently such biotinylated T7 bacteriophage particles were added to the magnetic nanoparticle solution. The resulting *ac* susceptibility measurements are shown in Fig. 5. Interestingly, the addition of biotinylated T7 bacteriophage results in the suppression of the susceptibility peak. This indicates that the magnetic nanoparticles are immobilized upon binding to the T7 bacteriophage, which is similar to the effect of freezing of the liquid in Fig. 4. The large phage particles with 415 copies of biotin molecules per phage effectively crosslink the avidin-coated magnetite nanoparticles, and thus causes their aggregation and immobilization.

The main advantage of the sensing scheme using the magnetic *ac* susceptibility is that the modification of Brownian relaxation offers an opportunity to distinguish between various possible targets. This is shown in Fig. 5 by changes in the frequency response upon binding to S-protein and biotinylated T7 bacteriophage. In the first case, the binding reaction results in a modified Brownian relaxation due to the increased hydrodynamic radius, while in the latter case the cross-linking of the magnetic nanoparticles with the bacteriophage suppresses the Brownian relaxation. Note that Weitschies *et al.* observed, via SQUID relaxometry, the change of Brown-to-Néel relaxation due to the immobilization of magnetic nanoparticles by biological binding activity [13, 27]. Although SQUID-based biosensors offer high sensitivity, they generally require more complex instrumentation than other sensing schemes due to the need for cryogens. Our sensing scheme operates at room temperature. Also, compared to other substrate-based sensors, it can be combined with subsequent magnetic high field-gradient separation since the particles remain in solution. Furthermore, since the magnetic nanoparticles exhibit a characteristic frequency peak even before binding to a target, our sensing scheme has an inherent check for its integrity. Table 1 summarizes a comparison of substrate-based stray field sensing, SQUID based sensing, and our substrate-free sensing scheme.

4. Conclusion

We have experimentally demonstrated a substrate-free biomagnetic sensing scheme using the Brownian relaxation of magnetic nanoparticles suspended in liquid. The binding of target molecules to magnetic nanoparticles changes the *ac* magnetic susceptibility response as a function of the frequency of an applied magnetic field. We performed the *ac* susceptibility measurements by magneto-optic as well as magneto-electric techniques. The advantage of this substrate-free sensing approach includes the additional information about the target size, the inherent integrity due to the presence of response signals with and without target molecules, and the possibility of subsequent magnetic separation.

Acknowledgement

The authors acknowledge helpful discussions with F.Y. Fradin. This work was supported by the U. S. Department of Energy, Basic Energy Sciences, under Contract No. DE-AC02-06CH11357.

References

[1] Gunter Schmid (Ed.), *Nanoparticles: from theory to application*, Wiley-VCH, Weinheim (2004).
[2] P. Tartaj, M. del Puerto Morales, S. Veintemillas-Verdaguer, T. Gonzalez-Carreno, and C. J Serna, J. Phys. D: Appl. Phys. **36**, R182 (2003).
[3] C. Liu, S.-H. Chung, Q. Jin, A. Sutton, F. Yan, A. Hoffmann, B. K. Kay, S. D. Bader, L. Makowski, and L. Chen, J. Magn. Magn. Mater. **302**, 47 (2006).
[4] Q. A. Pankhurst, J. Connolly, S. K. Jones, and J. Dobson, J. Phys. D: Appl. Phys. **36**, R167 (2003).
[5] P. Alivisatos, Nat. Biotechnol. **22**, 47 (2004).
[6] V. Labhasetwar, and D. L. Leslie-Pelecky (Ed.), *Biomedical applications of nanotechnology*, Wiley-InterScience, (in press).
[7] D. R. Baselt, G. U. Lee, M. Natesan, S. W. Metzger, P. E. Sheehan, and R. J. Colton, Biosens. Bioelectron. **13**, 731 (1998); R. L. Edelstein, C. R. Tamanaha, P. E. Sheehan, M. M. Miller, D. R. Baselt, L. J. Whitman, and R. J. Colton, *ibid.* **14**, 805 (2000).
[8] M. M. Miller, G. A. Prinz, S.-F. Cheng, and S. Bounnak, Appl. Phys. Lett. **81**, 2211 (2002).
[9] G. Li, V. Joshi, R. L. White, S. X. Wang, J. T. Kemp, C. Webb, R. W. Davis, and S. Sun, J. Appl. Phys. **93**, 7557 (2003); H. A. Ferreira, D. L. Graham, P. P. Freitas, and J.

M. S. Cabral, *ibid.* **93**, 7281 (2003).
[10] P.-A. Besse, G. Boreo, M. Demierre, V. Pott, and R. Popovic, Appl. Phys. Lett. **80**, 4199 (2002); G. Mihaloviæ, P. Xiong, S. von Molnár, K. Ohtani, H. Ohno, M. Field, and G. J. Sullivan, Appl. Phys. Lett. **87**, 112502 (2005).
[11] F. Ludwig, E. Heim, S. Mauselein, D. Eberbeck, and M. Schilling, J. Magn. Magn. Mater. **293**, 690 (2005).
[12] Y. R. Chemla, H. L. Grossman, Y. Poon, R. McDermott, R. Stevens, M. D. Alper, and J. Clarke, Proc. Natl. Acad. Sci. USA **97**, 14268 (2000).
[13] R. Kötitz. H. Matz, L. Trahms, H. Koch, W. Weitschies, T. Rheinlander, W. Semmler, and T. Bunte, IEEE Trans. Appl. Supercond. **7**, 3678 (1996); A. Haller, S. Hartwig, H. Matz, J. Lange, T. Rheinländer, R. Kötitz, W. Weitschies, and L. Trahms, Supercond. Sci. Technol. **12**, 956 (1999).
[14] J. Connolly, and T. G. St Pierre, J. Magn. Magn. Mater. **225**, 156 (2001).
[15] P. C. Fannin, B. K. P. Scaife, and S. W. Charles, J. Magn. Magn. Mater. **72**, 95 (1988).
[16] S. H. Chung, A. Hoffmann,, S. D. Bader, C. Liu, B. Kay, L. Makowski, and L. Chen, Appl. Phys. Lett **85**, 2971 (2004).
[17] A. Prieto Astalan, F. Ahrentorp, C. Johansson, K. Larsson, and A. Krozer, Biosens. Bioelectron. **19**, 945 (2004).
[18] M. I. Shliomis, Sov. Phys.-Usp. **17**, 153 (1974).
[19] S. H. Chung, A. Hoffmann, K. Guslienko, S. D. Bader, C. Liu, B. Kay, L. Makowski, and L. Chen, J. Appl. Phys. **97**, 10R101 (2005).
[20] F. Bødker, S. Mørup, and S. Linderoth, Phys. Rev. Lett. **72**, 282 (1994).
[21] Liquid Research, LTD, UK.
[22] Quantum Design, San Diego, CA, USA.
[23] S. H. Chung, M. Grimsditch, A. Hoffmann, S. D. Bader, J. Xie, S. Peng, and S. Sun, (unpublished).
[24] C. G. Granqvist and R. A. Buhrman, J. Appl. Phys. **47**, 2200 (1976).
[25] Novagen, Madison, WI, USA.
[26] N. M. Green, Adv. Protein Chem. **29**, 85 (1975).
[27] W. Weitschies, R. Kötitz, T. Bunte, and L. Trahms, Pharm. Pharmacol. Lett. **7**, 5 (1997).